KINETIC ENERGY CALCULATION AS AN AID TO INSTRUMENTATION LOCATION IN MODAL TESTING

Presented at
1990 MSC World Users Conference
March 1990
Los Angeles, California

Grant R. Parker
Ted L. Rose
The MacNeal-Schwendler Corporation
Los Angeles, California

John J. Brown
McDonnell Douglas Electronic Systems Company
Huntington Beach, California

KINETIC ENERGY CALCULATION AS AN AID TO INSTRUMENTATION LOCATION IN MODAL TESTING

Grant R. Parker
Ted L. Rose
The MacNeal-Schwendler Corporation
Los Angeles, California

John J. Brown
McDonnell Douglas Electronic Systems Company
Huntington Beach, California

ABSTRACT

MSC/NASTRAN provides the user with pre-coded programs, called rigid formats, that can be executed without having to learn the MSC/NASTRAN programming language. However, the program allows the user to write his own programs or alter existing MSC/NASTRAN rigid formats. This capability is called Direct Matrix Abstraction Programming (DMAP).

A number of papers have been written to illustrate the application of the kinetic energy calculation for mode shape identification utilizing the DMAP capability. This calculation has been utilized by industry for over ten years and has proven to be an invaluable tool. This paper expands the application to aid in identifying and selecting structural instrumentation locations for modal testing or for monitoring input/response during general and qualification vibration testing. The modal identification and instrument location procedures can be coupled to identify the modes of interest and then to select monitoring locations based on these modes. The DMAP is easily altered into the standard Normal Modes, Response, or Superelement rigid formats in MSC/NASTRAN and can be added to the standard SUBDMAP capability in Version 66 of the program.

Background on the approach plus unique (but not widely utilized) advantages offered by the kinetic energy calculation are presented along with a simple example. The power of the approach is realized in the effective display of results and the ability to quickly identify and select locations for test monitoring. This information, derived from the finite element analysis model of the structure, provides the test/analysis engineer with valuable, time-saving information.

KINETIC ENERGY CALCULATION AS AN AID TO INSTRUMENTATION LOCATION IN MODAL TESTING

Grant R. Parker
Ted L. Rose
The MacNeal-Schwendler Corporation
Los Angeles, California

John J. Brown
McDonnell Douglas Electronic Systems Company
Huntington Beach, California

INTRODUCTION

The modal kinetic energy calculation has proven to be a valuable tool to the analyst for mode shape identification and model checking. This paper expands the application to aid the analyst and test engineer in identifying and selecting structural instrumentation locations for modal testing, or for monitoring input/response during general and qualification vibration testing. MSC/NASTRAN provides the user with pre-coded programs, called Rigid Formats that can be executed without having to learn the MSC/NASTRAN programming language, called Direct Matrix Abstraction Programming (DMAP). This capability allows the user to write his own program or alter existing MSC/NASTRAN Rigid Formats.

In 1982, the authors published the paper "Kinetic Energy DMAP For Mode Identification" (Reference 1) which calculates the kinetic energy per degree-of-freedom per mode, and identifies the major contributors. This approach has received wide acceptance through the years. While the technique is used primarily for mode identification, results are also used for model checking. References 2 and 3 are examples of applications and extensions of the original work in mode identification in the automotive and aerospace industry. Reference 3 also introduces the separation of the motions and kinetic energy into their x-, y-, and z- scalar, and rotational components. This capability has added value in vibration testing, since sine and random testing are typically performed with excitation applied in one axis at a time for the three orthogonal

specimen axes. Responses are usually evaluated in terms of "in-line" or "cross-talk" response to these excitations. Reference 4 presents an excellent formulation of the kinetic energy calculation and provides an application of the approach for identifying the normal modes of a superelement model. The formulation from Reference 4 is presented in Appendix 1. As a quick review, the modal kinetic energy expression is based on a variation of certain orthogonal principles as shown in Equations 1 and 2.

$$\underset{NM \times DOF}{[\phi]^T} \quad \underset{DOF \times DOF}{[M]} \quad \underset{DOF \times NM}{[\phi]}$$

$$= \underset{NM \times NM}{[I]} = \text{Generalized Mass} \qquad (1)$$

$$\underset{NM \times DOF}{[\phi]^T} \quad \underset{DOF \times DOF}{[K]} \quad \underset{DOF \times NM}{[\phi]}$$

$$= \underset{NM \times NM}{[\omega^2]} = \text{Generalized Stiffness} \qquad (2)$$

where

$[\phi]$ is a matrix of orthonormalized modes

$[M]$ is the mass matrix

$[K]$ is the stiffness matrix

$[I]$ is an identity matrix

$[\omega^2]$ is the squared natural frequencies

DOF = degrees-of-freedom

NM = number of modes

A variation of Equation 1 forms the modal kinetic energy (KE) expression as shown in Equation 3.

$$\underset{DOF \times NM}{[\phi]} \quad \underset{E}{*} \quad \underset{DOF \times DOF}{[M]} \quad \underset{DOF \times NM}{[\phi]}$$

$$= \underset{DOF \times NM}{[KE]} \qquad (3)$$

where $\underset{E}{*}$ is a special element by element multiply.

Equations 1 and 2 produce square matrices in generalized, or modal coordinates (NM x NM), Equation 3 results in a rectangular matrix of discrete model coordinates by modes (DOF x NM), where detailed information is retained in terms of physical degrees-of-freedom for each mode.

Each element of a column of Equation 3 is equal to

$$KE_{ij} = \phi_{ij} \sum_{k=1}^{DOF} M_{ik} \phi_{kj} \qquad (4)$$

or the fraction of the total kinetic energy of the mode as a decimal, and the total kinetic energy of each column is equal to 1.0, i.e.:

$$KE_{j(TOTAL)} = \sum_{i=1}^{DOF} KE_{ij} = 1.0 \qquad (5)$$

This important **unity** relationship is made possible due to the unique properties of the orthonormalized modal matrix.

PRE-TEST ANALYSIS

New applications utilizing the modal kinetic energy calculation are now appearing as an aid to identifying monitoring locations for modal and dynamic testing. Efforts such as those presented in References 5, 6, and 7 also utilize the kinetic energy calculation and attempt, further, to optimize the placement of excitations and sensors. Reference 5 reviews the literature dealing with the placement of sensors in an optimal fashion and notes that none of the papers address the sensor placement problem from the standpoint of a structural dynamicist who must use the data collected from the sensors to validate a finite element model. The sensors must be placed such that the data collected during a vibration test will provide independent test mode shapes and frequencies that can be compared with finite element model (FEM) modal parameters using test-analysis correlation techniques (see Reference 8).

In Reference 6 it is noted that given "N" candidate locations for "M" sensors, there are N!/ M!(N-M)! possible combinations. Using typical finite element model sizes of ten thousand degrees-of-freedom, and

perhaps one hundred sensors available for monitoring response, one can quickly see the need for an automated procedure to aid in selecting locations. In discussing criterion for optimal placement of sensors, Reference 7 again points out that "if the sensing devices are accelerometers or strain gages, then locating them at degrees-of-freedom with the largest kinetic energy or strain energy will maximize the sensor's ability to efficiently observe the structural parameter of interest as well as changes thereof." The last statement about changes addresses the real goal of this paper, which is to begin a procedure (of which this paper is a first step) for **linking test and analysis results** that will be utilized for test-analysis correlation and finite element model update and improvement based on test data. This ability and other considerations, such as spatial effects, will be addressed in future work and will utilize the DMAP, normal modes, dynamic response, design sensitivity, and optimization capabilities in MSC/NASTRAN.

DISCUSSION

A recent article in Sound and Vibration, entitled "Using Finite Element Data to Set Up Modal Tests" (Reference 9), provided the background and impetus for this paper to provide an alternative approach for determining instrumentation location. In addition, the data recovery and data presentation outlined in the paper were quite useful. The next few paragraphs are largely extracted from that article. The introductory paragraph states: "Finite element analysis (FEA) mode shape data are available prior to many experimental modal analyses. Test engineers can make use of the FEA mode shape data to determine optimum test strategies. For example, the FEA mode shapes can be used to determine 'optimum' excitation and response locations in order to extract the modes of interest."

DRIVING POINT RESIDUES

The reference bases the selection of locations on a calculation of "**driving point residues (DPRs).**" DPRs are stated as being "equivalent to modal participation factors, and are a measure of how much each mode is excited, or participates in the overall response, at the driving point. DPRs are also proportional to the magnitudes of the resonance peaks in a driving point frequency response function

(FRF) measurement." The DPR (R being the residue) is defined for a lightly damped structure by equation 6 as:

$$R_k(a,a) \text{ (acc./force-sec.)} = u_k(a)^2\, \omega_k \quad \text{for } k = 1 \text{ to } N \tag{6}$$

where the FEA mode shape $\{u_k\}$ has been scaled to unit modal mass and the modal mass carries with it the units of (force-seconds^2/displacement).

To verify the DPR analysis technique presented in Reference 9, an FEA model was built for an 8 1/2 in. by 11 in. by 1/4 in. aluminum plate. The model was built with 88 quadrilateral plate elements, with three DOFs at each of the 108 grids or nodes: translation in the Z direction and rotations about the X and Y axes. The finite element model is shown in Figure 1. The first 10 modes of the structure were found from an eigensolution of the equations of motion, using free-free boundary conditions. The first three modes were rigid body modes and were not used the analysis. The first seven elastic modes were used in the DPR analysis. An actual plate was constructed and tested to compare results.

The Driving Point Residue (DPR) diagram in Figure 2 was generated from the FEA modes for the plate. Each vertical line of the diagram represents the range (minimum to maximum) and average value (designated by a '0') of the DPRs for the elastic modes 4 to 10, for a single DOF of the plate. In order to discriminate against those DOFs with zero DPRs, however, the vertical lines are ordered by a "weighted" average computed as:

weighted average = average DPR x minimum DPR

The lines are displayed beginning with the highest weighted average (best driving point) on the left side over to the lowest weighted average (worst driving point) on the right. (An entire DPR diagram for the plate has 108 lines, but only the 64 best lines are shown in Figure 2.) The DPR diagram shows that, of the 64 best driving points, DOF 45Z is one of the poorer choices (second from the right). The DPR diagram also shows that DOF 1Z is one of the best driving points. Figures 1 and 2 were copied from Reference 9.

Finally, to check the validity of the method, a test was performed on an aluminum plate. Frequency Response Functions (FRF) were measured and curve fitted to allow comparison of measured residues with those computed from the FEA data. Comparison of analytical

and experimental DPRs was good. Actual results can be obtained from the reference if desired.

KINETIC ENERGY DMAP CALCULATION

The objective of this paper is to replace the use of the DPR calculation with that of the Kinetic Energy Calculation. To accomplish this objective, the rectangular plate analysis has been repeated in MSC/NASTRAN using both the DPR approach and the Kinetic Energy Calculation. As a first step, Equation 6 for the DPR calculation was written as a DMAP in MSC/NASTRAN. The DMAP was written for use in Version 66 of MSC/NASTRAN and has been annotated with comments to assist the user in following the program. The plate model of Figure 1 was reconstructed using MSC/XL and is shown in Figure 3. The Data Deck for the Test Plate Problem is shown in Figure 4. The DMAP is added through an "INCLUDE" command, and the analysis output data is accessed from the "OUTPUT4" module using the "ASSIGN" command. The BULK DATA section has been truncated to show only the necessary model information. The data deck is sent directly from MSC/XL to MSC/NASTRAN for processing.

The DMAP alters for Solution 103 for performing the DPR and the Kinetic Energy Calculations are shown in Figure 5 and were written for the Kinetic Energy expression in Equation 3. This DMAP utilizes the "SUBDMAP" capabilities offered in Version 66.

Figure 6 presents the eigenvalue table from the MSC/NASTRAN output. The first three modes are rigid body modes followed by 7 elastic modes. Table 1 shows the Minimum, Maximum, and Average DPR values as calculated by the DMAP. These results are presented graphically in Figure 7. The last column in Table 1 (ORDER) correlates the abscissa values in Figure 7. Grid points with the highest average are 12, 108, 1, 97, etc. They are ranked, from left to right, by the largest "weighted average" values. These results compare with the results in Reference 9, as shown in Figure 2 which uses a semi-log presentation. The display of Figure 7 was constructed using the Lotus Symphony PC program and the OUTPUT4 data from MSC/NASTRAN.

The Kinetic Energy Calculation data from the DMAP is shown in Table 2. Figure 8 presents the data as sorted by "weighted average"

similar to the DPR plot of Figure 7. Figure 9 presents the data as sorted by the average (unweighted) value. Again, the last column in Table 2 correlates the abscissa values noted on the figures.

As mentioned, the SUBDMAP capability can be utilized to partition the responses of interest, i.e., X, Y, and Z, for evaluating directions correlating to test inputs. This capability should prove to be very beneficial in locating instrumentation.

RESULTS

Differences occured between the two approaches, as expected, since the DPR calculation does not include the effects of the mass matrix. The DPR calculation selected the four corners of the plate as the most desirable input/output response locations. Figure 2 has ranked these grid points first. The Kinetic Energy calculation selected grid points 13, 24, 85, and 96 based on average values, but picked the same first four points (only) as the DPR calculation using the weighted averages. Choices for maximum values differed between the two approaches. A close comparison of Tables 1 and 2 and Figures 2, 6, and 7 shows other differences in the results of the two approaches. Clearly, the use of the mass matrix (and its formulation) accounts for the difference.

The value of the display is evident in the ability to quickly identify candidate points for locating sensors.

The following question arises: which procedure should be followed? It is suggested that since the mass data is available from the analysis, it would seem reasonable to utilize this information. It is felt that the different approaches are typical of the different backgrounds of the analyst and tester. Since engineers working with experimental data do not usually work with finite element model data, they are normally forced to work with the available measured data, which does not include a mass matrix. Industry is proceeding towards a merging of the two disciplines, which will benefit us all. The test engineers have paved the way in technology development which is now being acknowledged and utilized by the analysis (finite element) community. While the differences for this example are minor and explainable, the results could differ significantly in more complex structural models.

FOLLOW-ON WORK

Due to time constraints, the approach was not applied to a larger, three-dimensional structure such as the disk drive deck plate structure in Reference 9. This and other more complex structures will be investigated in future work. In addition, a comprehensive DMAP is available that provides the calculations for superelement models as well. The ability to partition response directions in the X, Y, and Z is included, but was not demonstratable in the simple plate example since there was only one translational degree-of-freedom. Other checks, presented in Reference 4, are also included in the comprehensive DMAP. An alter for Version 65C is also available. Applications will be sought to compare actual test data based on sensor locations provided by this DMAP, and will be used for model refinement based on design sensitivity and optimization capabilities in MSC/NASTRAN.

CONCLUSION

This paper has highlighted an alternate approach for using finite element data based upon the Kinetic Energy Calculation to set up modal tests, and has utilized the valuable methodology and results display of Reference 9. Reference 3 points out that the analyst and tester must avail themselves of as much information as possible to guide their decisions. Mode shapes must also be carefully reviewed in the selection process. Future work utilizing the DMAP capabilities in MSC/NASTRAN has also been outlined.

ACKNOWLEDGEMENT

The authors wish to express their thanks to Bill Moffitt of MSC for his assistance in preparing the paper.

REFERENCE

1. Parker, G. , Brown, J. , "Kinetic Energy DMAP for Mode Identification," MSC/NASTRAN USERS CONFERENCE PROCEEDINGS, Pasadena, CA, March, 1982.

2. Brown, J. , Parker, G. , "An Application of the Kinetic Energy Calculation as an Aid in Mode Identification," The Shock And Vibration Bulletin, May 1983.

3. Schwering, S. , "A DMAP for Identification of Modeshapes," PROCEEDINGS OF THE MSC/NASTRAN EUROPEAN USERS CONFERENCE, Munich, West Germany, June, 1983.

4. Rose, T. , "Using Superelements To Identify the Dynamic Properties of a Structure," MSC/NASTRAN USERS CONFERENCE PROCEEDINGS, Universal City, CA, March, 1988.

5. Kammer, D. , "Sensor Placement for On-Orbit Modal Identification and Correlation of Large Space Structures," Accepted for publication in AIAA Journal of Guidance, Control, and Dynamics, 1990.

6. Lim, T. , Cooper, P. "Optimization of Sensor Placement Using Internal Balancing theory and Simulated Annealing," NASA LaRC presentation, October 1989.

7. Salma, M. , Rose, T. , Garba, J. , "Optimal Placement Of Excitations and Sensors For Verification of Large Dynamical Systems," AIAA Paper #87-0782, 1987.

8. Kammer, D. , "Test-Analysis Correlation of the Space Shuttle Solid Rocket Motor Center Segment," Journal of Spacecraft, Vol. 26, No. 4, March 1988.

9. Kientzy, D. , Richardson, M. , Blakely, K. , "Using Finite Element Data to Set Up Modal Tests," Sound and Vibration, June 1989.

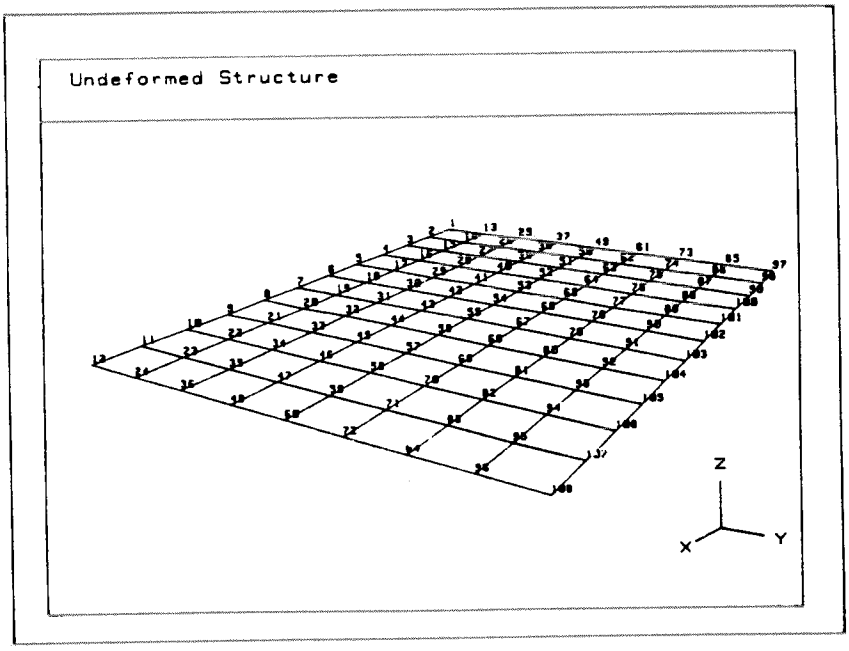

Figure 1. Finite element model of the flat plate.

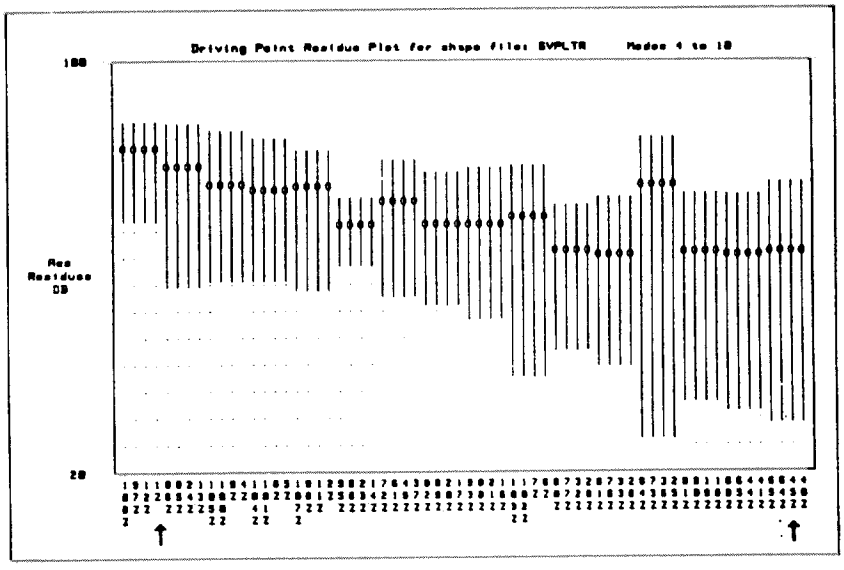

Figure 2. DPR diagram for the flat plate.

FIGURES 1 and 2 from Reference 9

PLATE MODEL

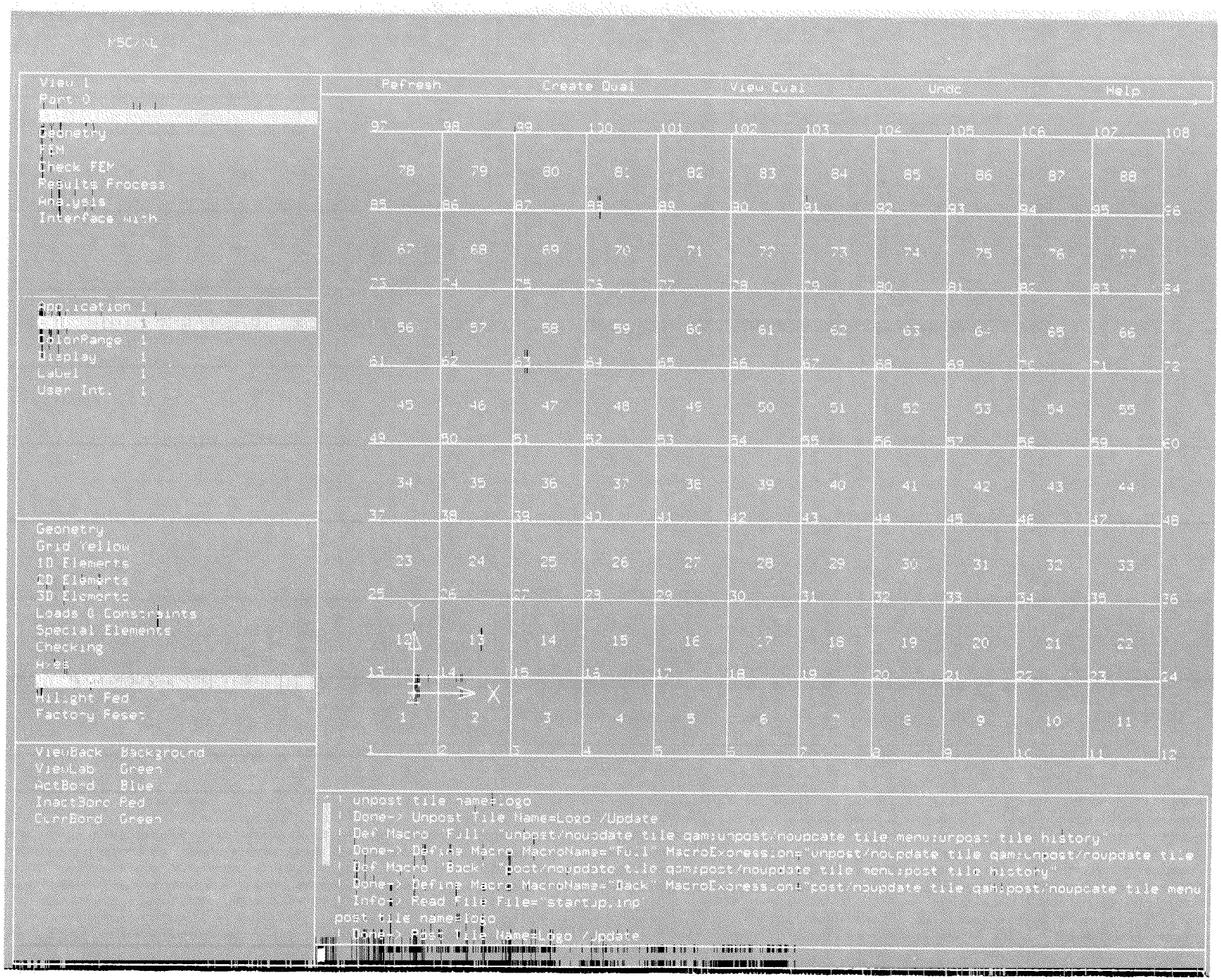

FIGURE 3

DATA DECK FOR THE TEST PLATE PROBLEM

(NOTE "INCLUDE" STATEMENTS FOR ALTERS)

```
ASSIGN OUTPUT4=EAD:[TLR.VER66]TESTPLATE.F12,NEW,UNIT=12,    FORMATTED $
ASSIGN OUTPUT4=EAD:[TLR.VER66]TESTPLATE.F13,NEW,UNIT=13,    FORMATTED $
ID SE, SAMPLE PROBLEM - SOL 103 NO S E
SOL 103
DIAG 8
TIME 15
INCLUDE   EAD:[TLR.VER66]UC90.DAT
CEND
TITLE = S.E. SAMPLE PROBLEM 1
SUBTITLE = NORMAL MODES USING SOL 103 - NO S.E.
METHOD = 1
DYNRED = 1
DISP = ALL
BEGIN BULK
DEFUSET,U1,U1,U2,U2,U3,U3,U4,U4,+DEFU
+DEFU,U5,U5,U6,U6
USET1,U1,1,1,THRU,108
USET1,U2,2,1,THRU,108
USET1,U3,3,1,THRU,108
USET1,U4,4,1,THRU,108
USET1,U5,5,1,THRU,108
USET1,U6,6,1,THRU,108
$
$
$ THIS SECTION CONTAINS BULK DATA FOR PART 0 SUPERELEMENT 0
$
$
EIGRL,1,,,10
GRDSET,,,,,,,126
GRID     1       0       0.0     0.0     0.0
GRID     2       0       1.      0.0     0.0
GRID     3       0       2.      0.0     0.0
GRID     4       0       3.      0.0     0.0
GRID     5       0       4.      0.0     0.0
  .
  .   (GRID AND QUAD4 BULK DATA SKIPPED)
  .
CQUAD4   88      1       95      96      108     107
$
$ THIS SECTION CONTAINS THE PROPERTY AND MATERIAL BULK DATA ENTRIES
$
PSHELL   1       1       .25     1
$
PARAM,WTMASS,.00259
MAT1     1       1.+7            .33     .1
PARAM    POST    0
PARAM    AUTOSPC YES
ENDDATA
```

FIGURE 4

```
$
$ ALTER TO COMPUTE KINETIC ENERGY AND DPR FOR
$          FOR VERSION 66
$
$
$
$ MODIFY SEDRCVR - ADD CALLS FOR KE AND DPR
$
$
COMPILE SEDRCVR SOUIN=MSCSOU $
ALTER 109      $          AFTER OFP  OUGV1,OPG1,.......
CALL KEEFW UGVS/TEST99/SEID $
$
$
$ SUBDMAP KEEFW - CALCULATE KE AND DPR
$
COMPILE KEEFW $
SUBDMAP KEEFW UGVS1/TEST99/SEID $
$
$ SUBDMAP KEEFW - CALCULATE KE AND EFW IF REQUESTED
$
TYPE DB,EQEXINS,GPLS,SILS,USET,MGG,ZUZR02,MJJ,ZUZR01 $
TYPE PARM,NDDL,I,N,SEID,LUSETS,PEID $
TYPE PARM,,I,N,(LUSETD) $
TYPE PARM,,I,Y,(KEPRT=0,EFWGT=-1,KEEFW=1) $
TYPE PARM,NDDL,I,N,NOUP,ZUZR1,ZUZR2,ZUZR3,PEID $
TYPE PARM,NDDL,RS,Y,(WTMASS) $
TYPE PARM,,RS,N,(MW) $
TYPE PARM,,CS,Y,(MASSWT) $
TYPE PARM,,I,N,MODENO,MOLEFT,MODNOM1,MOLEFT $ ***
TYPE PARM,,CS,N,,FREQIN $ ***
TYPE DB,BGPDTS,CSTMS,LAMA,CASES $ ****
$
DBVIEW CASEP=CASES (WHERE SEID=PEID)  $    CASE CONTROL CARD
PARAML CASEP//'DTI'/1/8//S,N,MTEMP $    TEMP(MAT)
PARAML CASEP//'DTI'/1/2//S,N,MPC $      MPC
PARAML CASEP//'DTI'/1/3//S,N,SPC $      SPC
PARAML CASEP//'DTI'/1/185////S,N,K2GG $ K2GG
PARAML CASEP//'DTI'/1/187////S,N,M2GG $ M2GG
PARAML CASEP//'DTI'/1/150//S,N,DYRD $   DYNRED
PARAML CASEP//'DTI'/1/5  //S,N,METH $   EIGR OR EIGRL
$
IF(WTMASS=0.)WTMASS=1. $
MW=1./WTMASS $
MASSWT=CMPLX(MW,0.) $
$
$ AFTER SDR1 - SYSTEM K.E.
$
```

FIGURE 5

```
$ ALTER TO COMPUTE KINETIC ENERGY AND DPR FOR
$         FOR VERSION 66


$
 IF (KEPRT>-1)THEN $ REQUEST MADE FOR KE AND DPR
  ZUZR1=SEID $
    MPYAD UGVS1,MGG,/PHITM/1//// $
       TRNSP PHITM/PHITMT $
       ADD PHITMT,UGVS1/ENERGWUP///1 $
          MATGEN EQEXINS/INTEXT/9/0/LUSETS $
          MPYAD  ENERGWUP,INTEXT,/ENUPEX/1 $
          TRNSP ENUPEX/ENUPEXT $
          OUTPUT4 ENUPEXT///13/0 $WRITE TO FILE 12
       MPYAD PHITM,UGVS1,/TOTEN1/ $
       DIAGONAL TOTEN1/TOTENWUP $
       MATPRN TOTENWUP// $
       MATGPR GPLS,USET,SILS,ENERGWUP//'H'/'G'//1.-2 $ 1%
$ FILTER ON ENERGY
       LAMX  ,,LAMA/LAMAT/-1 $
       MATGEN ,/CPLAMA/6/5/0/1/4 $
       PARTN LAMAT,CPLAMA,/,,EIGVAL,/1 $
       MATGEN ,/CPLAMA1/6/5/1/1/3 $
       PARTN LAMAT,CPLAMA1,/,,OMEGA,/1 $
$
$  CALC VALUES FROM RICHARDSON EQ 20
$
$
$    PLACE EIGENVECTOR INTO EXTERNAL SORT
$
        MPYAD  UGVS1,INTEXT,/UGVEX/1 $
        TRNSP UGVEX/UGVEXT $
$  FIRST CALC PHI**2
        ADD UGVEXT,UGVEXT/PHISQ///1 $
$
$  PEEL OFF ONE COLUMN (MODE) AT A TIME AND MULTIPLY BY THE
$  FREQUENCY
$
        PARAML PHISQ//'TRAILER'/1/S,N,NMODES $
        PARAML PHISQ//'TRAILER'/2/S,N,NDOF $
        MATGEN ,/UNITVEC/6/NDOF/0/NDOF $ UNIT VECTOR
        MODENO=1 $
        FILE PHISQW=APPEND $
        DO WHILE (MODENO<=NMODES) $
          MODNOM1=MODENO-1 $
          MOLEFT = NMODES-MODENO $
```

FIGURE 5 (CONTINUED)

```
$ ALTER TO COMPUTE KINETIC ENERGY AND DPR FOR
$          FOR VERSION 66


$  GENERATE PARTITIONING VECTOR TO GET CURRENT MODE
           MATGEN ,/CPMODE/6/NMODES/MODNOM1/1/MOLEFT $
           PARTN PHISQ,CPMODE,/,,ONEMODE,/1 $ MODE SHAPE
           SCALAR OMEGA//MODENO/1/S,N,FREQ $ GET CURRENT FREQ
$ AS A PARAMETER
           FREQIN=FREQ/MASSWT $
           ADD UNITVEC,ONEMODE/RESULT/FREQIN//1 $
           APPEND RESULT,/PHISQW/2 $
           MODENO = MODENO + 1 $
         ENDDO $
         OUTPUT4 PHISQW///12/0 $WRITE TO FILE 12
  ENDIF $
  $
  $
RETURN $
END $
$
```

FIGURE 5 (CONTINUED)

NORMAL MODES USING SOL 103 - NO S.E.

R E A L E I G E N V A L U E S

MODE NO.	EXTRACTION ORDER	EIGENVALUE	RADIANS	CYCLES	GENERALIZED MASS	GENERALIZED STIFFNESS
1	1	-2.719462E-07	5.214846E-04	8.299685E-05	1.000000E+00	-2.719462E-07
2	2	-2.142042E-07	4.628220E-04	7.366041E-05	1.000000E+00	-2.142042E-07
3	3	-1.676381E-08	1.294751E-04	2.060660E-05	1.000000E+00	-1.676381E-08
4	4	4.294496E+06	2.072316E+03	3.298194E+02	1.000000E+00	4.294496E+06
5	5	6.471600E+06	2.543934E+03	4.048796E+02	1.000000E+00	6.471600E+06
6	6	1.971841E+07	4.440542E+03	7.067342E+02	1.000000E+00	1.971841E+07
7	7	2.391385E+07	4.890179E+03	7.782961E+02	1.000000E+00	2.391385E+07
8	8	3.312872E+07	5.755755E+03	9.160568E+02	1.000000E+00	3.312872E+07
9	9	5.469047E+07	7.395301E+03	1.176999E+03	1.000000E+00	5.469047E+07
10	10	8.542071E+07	9.242333E+03	1.470963E+03	1.000000E+00	8.542071E+07

FIGURE 6

DPR RESULTS TABLE

GRID	DOF	MAX	MIN	AVG	WGT AVG	ORDER
12	3	24283.5	2564.813	13498.46	34621035	1
108	3	24283.5	2564.813	13498.46	34621035	2
1	3	24283.5	2564.813	13498.46	34621035	3
97	3	24283.5	2564.813	13498.46	34621035	4
96	3	24321.49	620.4208	8968.384	5564172.	5
85	3	24321.49	620.4208	8968.384	5564172.	6
13	3	24321.49	620.4208	8968.384	5564172.	7
24	3	24321.49	620.4208	8968.384	5564172.	8
100	3	19813.95	711.4991	5863.186	4171651.	9
105	3	19813.95	711.4991	5863.186	4171651.	10
9	3	19813.95	711.4991	5863.186	4171651.	11
4	3	19813.95	711.4991	5863.186	4171651.	12
101	3	16277.02	689.3162	5132.643	3538014.	13
5	3	16277.02	689.3162	5132.643	3538014.	14
104	3	16277.02	689.3162	5132.643	3538014.	15
8	3	16277.02	689.3162	5132.643	3538014.	16
107	3	13042.13	524.2626	5613.190	2942785.	17
2	3	13042.13	524.2626	5613.190	2942785.	18
11	3	13042.13	524.2626	5613.190	2942785.	19
98	3	13042.13	524.2626	5613.190	2942785.	20
14	3	4361.734	955.3425	2367.539	2261810.	21
23	3	4361.734	955.3425	2367.539	2261810.	22
95	3	4361.734	955.3425	2367.539	2261810.	23
86	3	4361.734	955.3425	2367.539	2261810.	24
37	3	9990.836	478.9943	4052.694	1941217.	25
48	3	9990.836	478.9943	4052.694	1941217.	26
72	3	9990.836	478.9943	4052.694	1941217.	27
61	3	9990.836	478.9943	4052.694	1941217.	28
20	3	7762.315	393.4529	2391.419	940910.8	29
92	3	7762.315	393.4529	2391.419	940910.8	30
17	3	7762.315	393.4529	2391.419	940910.8	31
89	3	7762.315	393.4529	2391.419	940910.8	32
88	3	8644.635	295.7277	2392.164	707429.1	33
93	3	8644.635	295.7277	2392.164	707429.1	34
21	3	8644.635	295.7277	2392.164	707429.1	35
16	3	8644.634	295.7277	2392.163	707429.1	36
102	3	8959.21	79.2683	2817.242	223318.0	37
6	3	8959.21	79.2683	2817.242	223318.0	38
7	3	8959.21	79.2683	2817.242	223318.0	39
103	3	8959.21	79.2683	2817.242	223318.0	40
98	5	14740.9	52.17544	3569.898	186261.0	41

TABLE 1

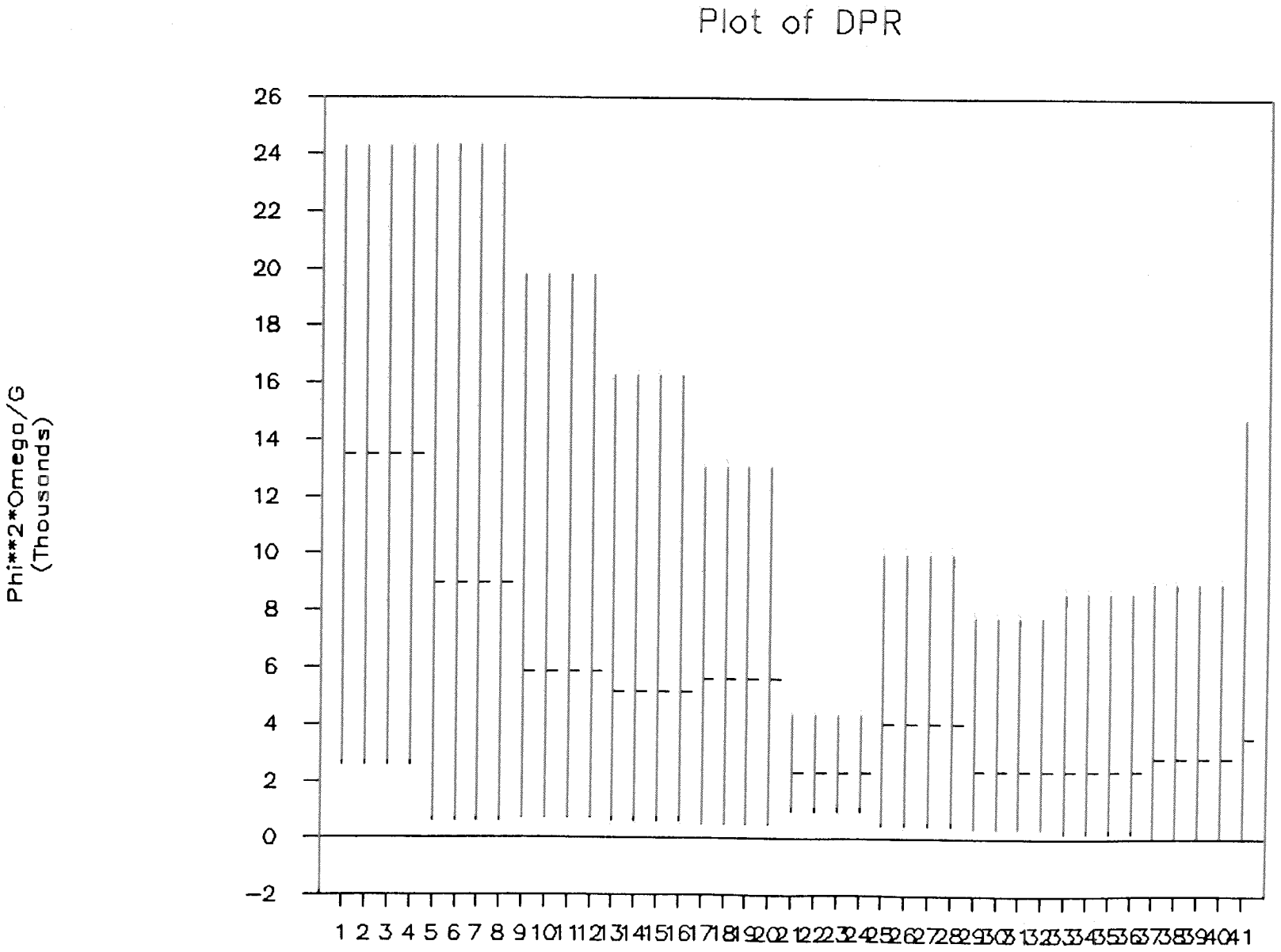
Plot of DPR
Phi**2*Omega/G
(Thousands)
26
24
22
20
18
16
14
12
10
8
6
4
2
0
-2
1 2 3 4 5 6 7 8 9 10 11 12 13 14 15 16 17 18 19 20 21 22 23 24 25 26 27 28 29 30 31 32 33 34 35 36 37 38 39 40 41

FIGURE 7

KINETIC ENERGY RESULTS TABLE

GRID	DOF	MAX	MIN	AVG	WGT AVG	ORDER
1	3	0.023429	0.006695	0.016609	0.000111	1
108	3	0.023429	0.006695	0.016609	0.000111	2
12	3	0.023429	0.006695	0.016609	0.000111	3
97	3	0.023429	0.006695	0.016609	0.000111	4
95	3	0.035586	0.006280	0.014992	0.000094	5
14	3	0.035586	0.006280	0.014992	0.000094	6
86	3	0.035586	0.006280	0.014992	0.000094	7
23	3	0.035586	0.006280	0.014992	0.000094	8
101	3	0.023390	0.004417	0.011605	0.000051	9
5	3	0.023390	0.004417	0.011605	0.000051	10
8	3	0.023390	0.004417	0.011605	0.000051	11
104	3	0.023390	0.004417	0.011605	0.000051	12
89	3	0.022308	0.003344	0.010512	0.000035	13
20	3	0.022308	0.003344	0.010512	0.000035	14
92	3	0.022308	0.003344	0.010512	0.000035	15
17	3	0.022308	0.003344	0.010512	0.000035	16
24	3	0.034950	0.001431	0.021115	0.000030	17
96	3	0.034950	0.001431	0.021115	0.000030	18
85	3	0.034950	0.001431	0.021115	0.000030	19
13	3	0.034950	0.001431	0.021115	0.000030	20
4	3	0.028472	0.002250	0.012892	0.000029	21
100	3	0.028472	0.002250	0.012892	0.000029	22
9	3	0.028472	0.002250	0.012892	0.000029	23
105	3	0.028472	0.002250	0.012892	0.000029	24
61	3	0.024872	0.002260	0.010731	0.000024	25
72	3	0.024872	0.002260	0.010731	0.000024	26
37	3	0.024872	0.002260	0.010731	0.000024	27
48	3	0.024872	0.002260	0.010731	0.000024	28
88	3	0.024844	0.001973	0.010150	0.000020	29
21	3	0.024844	0.001973	0.010150	0.000020	30
16	3	0.024844	0.001973	0.010150	0.000020	31
93	3	0.024844	0.001973	0.010150	0.000020	32
11	3	0.030130	0.000952	0.016689	0.000015	33
2	3	0.030130	0.000952	0.016689	0.000015	34
98	3	0.030130	0.000952	0.016689	0.000015	35
107	3	0.030130	0.000952	0.016689	0.000015	36
18	3	0.026120	0.000578	0.007729	0.000004	37
19	3	0.026120	0.000578	0.007729	0.000004	38
90	3	0.026120	0.000578	0.007729	0.000004	39
91	3	0.026120	0.000578	0.007729	0.000004	40
6	3	0.024332	0.000508	0.008301	0.000004	41

TABLE 2

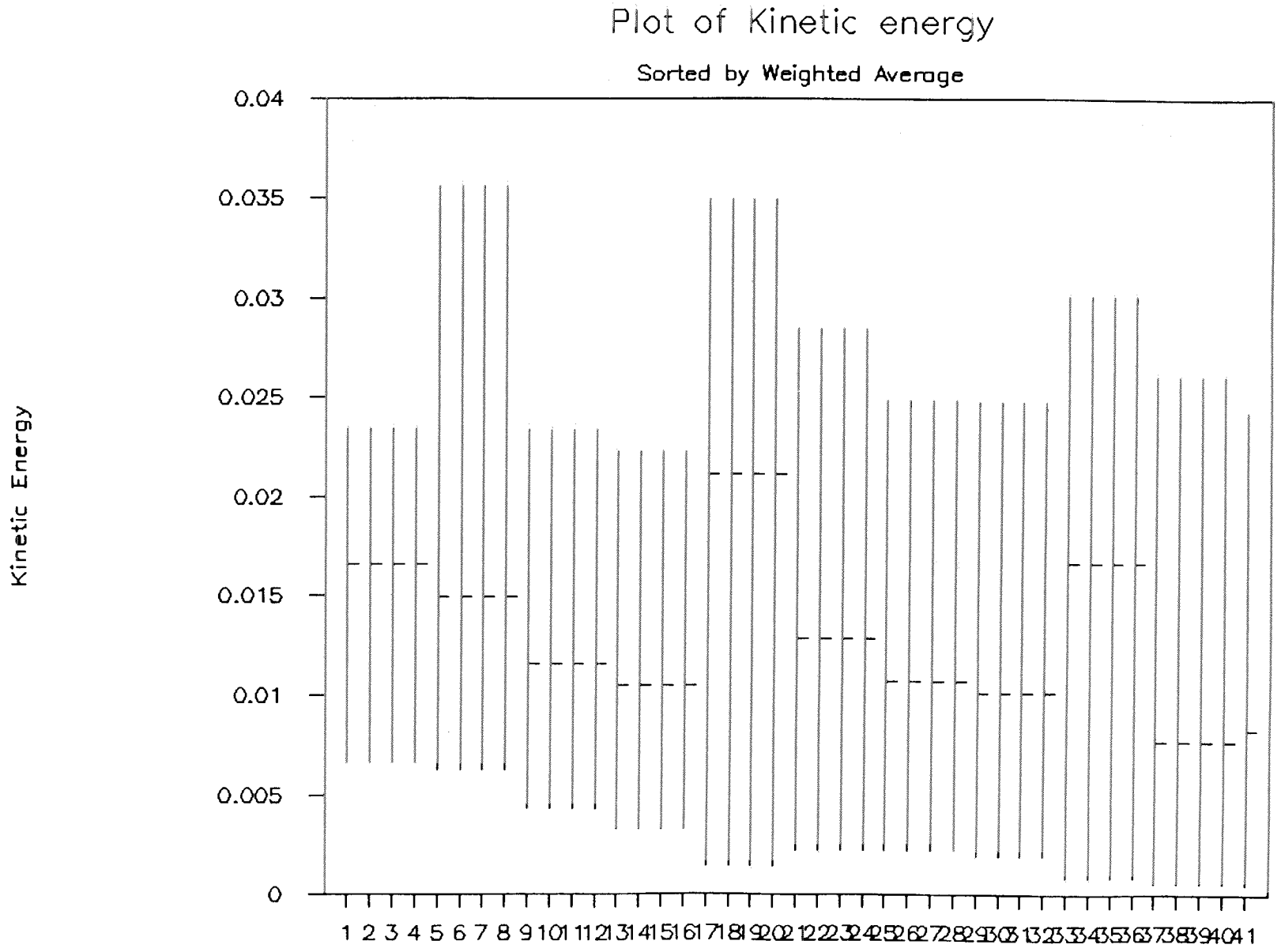
Plot of Kinetic energy
Sorted by Weighted Average
Kinetic Energy
0.04
0.035
0.03
0.025
0.02
0.015
0.01
0.005
0
1 2 3 4 5 6 7 8 9 10 11 12 13 14 15 16 17 18 19 20 21 22 23 24 25 26 27 28 29 30 31 32 33 34 35 36 37 38 39 40 41

FIGURE 8

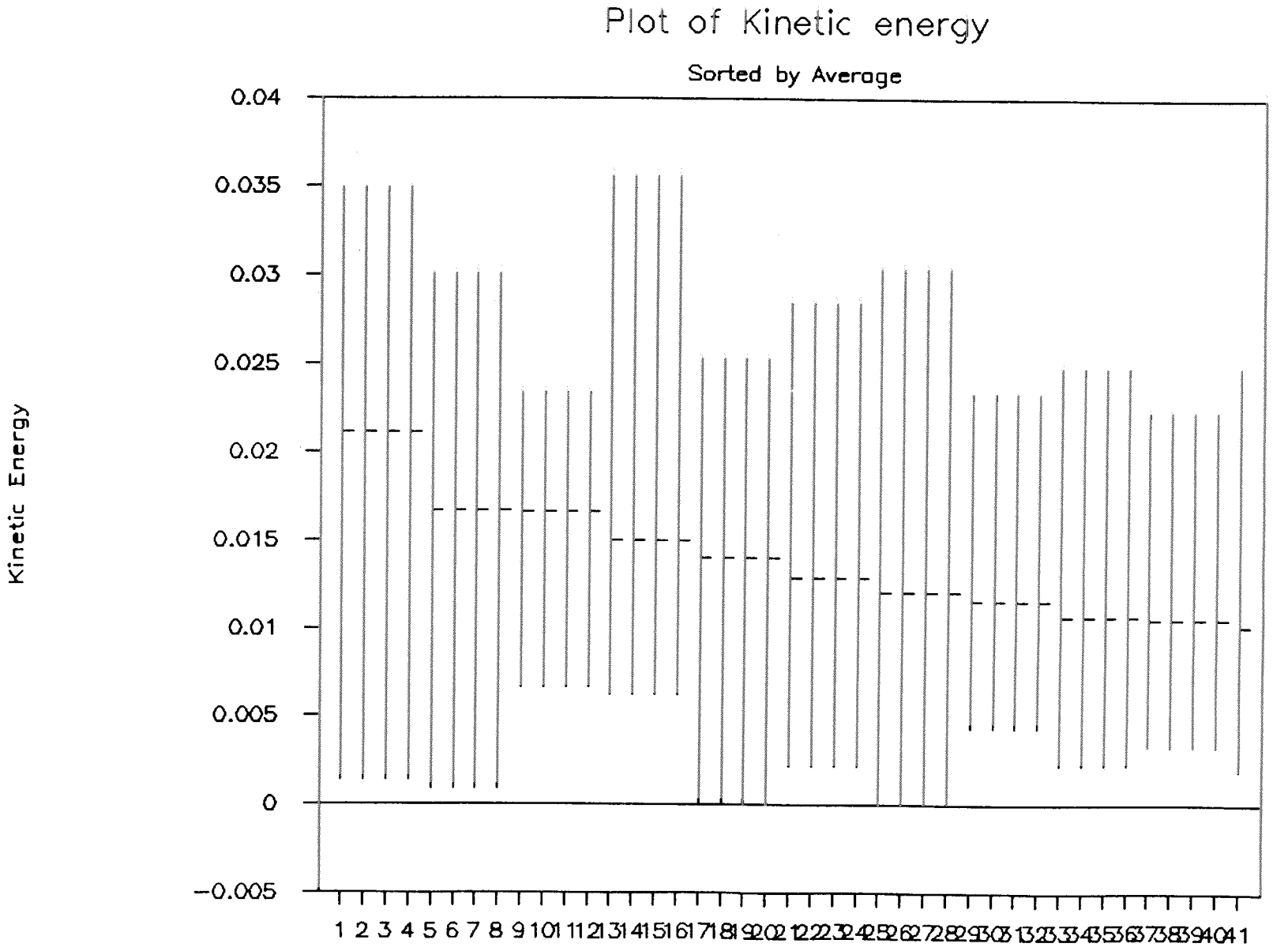
Plot of Kinetic energy
Sorted by Average
Kinetic Energy
0.04
0.035
0.03
0.025
0.02
0.015
0.01
0.005
0
-0.005
1 2 3 4 5 6 7 8 9 10 11 12 13 14 15 16 17 18 19 20 21 22 23 24 25 26 27 28 29 30 31 32 33 34 35 36 37 38 39 40 41

FIGURE 9

APPENDIX

Kinetic Energy

The expression normally used for kinetic energy is:

$$K.E. = \frac{1}{2} mv^2$$

for a point mass, m, moving with velocity, v. The kinetic energy for a system is the sum of all its components. In a finite element model, the mass is represented in matrix form utilizing the degrees of freedom at the grid points in the mass matrix [M]. This matrix is normally formed using the lumped mass assumption, that is, there are no off-diagonal terms in the matrix. In this situation, the method given in this paper is exact for the model. If the mass matrix is not diagonal, the method is an approximate, but, based on past experience, appears to work quite well.

The Alter uses the following method to calculate kinetic energy. The displacement $x_{i,n}(t)$ of any degree of freedom i in a specified mode n can be represented as

$$x_{i,n}(t) = a_{i,n} \sin \omega_n t \qquad (1)$$

where $a_{i,n}$ is the modal displacement of d.o.f. i in mode n and ω_n is the frequency of mode n.

The velocity is simply the first derivative of displacement with respect to time, or

$$v_{i,n}(t) = a_{i,n}\,\omega_n \cos\omega_n t \tag{2}$$

thus, with mass, m_i, associated with d.o.f. i, the kinetic energy at d.o.f. i is,

$$k.e._{i,n} = \frac{1}{2} m_i v_i^2 = \frac{1}{2} m_i\, a_{i,n}^2\, \omega_n^2 \cos^2\omega_n t \tag{3}$$

On a system level, the kinetic energy of the system for mode n is

$$K.E._n = \sum_{i=1}^{ndof} \frac{1}{2} m_i\, a_{i,n}^2\, \omega_n^2 \cos^2 \omega_n t \tag{4}$$

$$= \frac{1}{2}\omega_n^2 \cos^2\omega_n t \sum_{i=1}^{ndof} m_i a_{i,n}^2 \tag{5}$$

this can be shown in matrix form as

$$K.E._n = \frac{1}{2}\omega_n^2 \cos^2\omega_n t \,\{\phi_n\}^T [m_i] \{\phi_n\} \tag{6}$$

where

$$\{\phi_n\} = \begin{Bmatrix} a_{1,n} \\ a_{2,n} \\ a_{3,n} \\ \vdots \\ a_{ndof,n} \end{Bmatrix}$$

is the vector (mode shape) for mode n and

$$[m_i]$$

is a diagonal matrix containing the masses associated with the d.o.f.

At this point, it can be noted that the mode shapes are non-dimensional quantities and can be scaled in any number of ways. Due to this, it is best to scale the kinetic energy of the individual d.o.f.'s by the total to get a number which represents the portion of the total system K.E. at each d.o.f. This is accomplished by dividing equation (3) by equation (6), which gives

$$\text{K.E. Fraction}_{i,n} = \frac{\text{k.e.}_{i,n}}{\text{K.E.}_n} = \frac{\frac{1}{2} m_i a_{i,n}^2 \omega_n^2 \cos^2 \omega_n t}{\frac{1}{2} \omega_n^2 \cos^2 \omega_n t \{\phi_n\}^T [m_i] \{\phi_n\}} \tag{7}$$

or,

$$\text{KEFraction}_{i,n} = \frac{m_i a_{i,n}^2}{\{\phi_n\}^T [m_i] \{\phi_n\}} \tag{8}$$

In the case where we normalize the modes to unit mass,

$$\{\phi_n\}^T [m_i] \{\phi_n\} = 1.0 \tag{9}$$

Combining equations (8) and (9) gives,

$$\text{KEFraction}_{i,n} = m_i a_{i,n}^2 \tag{10}$$

for any d.o.f. i, if the mass matrix is diagonal and the modes are scaled to unit mass.

The kinetic energy fractions for all of the d.o.f. in the model can be obtained in matrix form by

$$\{\text{KEFraction}\}_n = \{\phi_n\}^T [m] \cdot \{\phi_n\} \tag{11}$$

where the $\cdot$ means perform a term-by-term multiply as opposed to a matrix multiply.

The kinetic energy fraction can be obtained for all of the modes by using

$$\{\phi\} = \{\phi_1 : \phi_2 : \phi_3 : \phi_4 : \cdots \phi_{n \text{ modes}}\} \tag{12}$$

in equation 11, or

$$\{\text{KEFraction}\} = \{\phi\}^T [m] \cdot \{\phi\}$$

where each column of the KEFraction matrix represents one mode.

The explanation so far has concentrated on models with a diagonal mass matrix. As it turns out, the results of having a coupled mass matrix (such as one resulting from performing a Guyan reduction) appear to be equally as good.